DSPACE

https://dspace.org/

Physicochemical properties of smoke generated particles during chrcolbased meat preparation in an informal restaurat in the city of Joburg

MD Masekameni; PC Rathebe; Thobelani Khumalo

https://hdl.handle.net/10539/48415
SCOPUS

Downloaded from a DSpace repository. https://dspace.org/

Research article

Physicochemical properties of smoke generated particles during charcoal-based meat preparation in an informal restaurant in the city of Johannesburg

Masilu Daniel Masekameni[1*], **Thobelani S Khumalo**[2], **Phoka Caphus Rathebe**[3]

[1]Development Studies, School of Social Sciences, University of South Africa, South Africa
[2]Occupational Health Division, School of Public Health Faculty of Health Sciences, University of the Witwatersrand, South Africa
[3]Department of Environmental Health, Faculty of Health Sciences, University of Johannesburg, South Africa
*Corresponding author: maseksd@unisa.ac.za

Received: 27 February 2024 - **Reviewed:** 21 May 2024 - **Accepted:** 4 July 2025
https://doi.org/10.17159/caj/2025/35/2.17606

Abstract

This study investigated the physicochemical properties of particles generated from different combustion phases (viz. ignition, flaming and coking). A total of three chicken grilling/ braaiing stalls were selected for physicochemical profiles of charcoal combustion particles. The samples were collected 1.5 m above the ground and 0.8 m away from the stove. Samples were collected in triplicate to minimize uncertainty making a total of 27 data points (in triplicates) for studying particle size distribution, mass and number concentration. Monitoring of particles was done using a real-time Nanozen DustCount 9000 Personal Dust Monitor. Samples for chemical assessments were collected on 37 mm PVC filters with a pore size of 5 µm. A Gilair pump at a flow rate of 2.2 l/minute was used to draw in the air over a monitoring campaign of 2 hours and 20 minutes per burning cycle. A $PM_{2.5}$ cyclone with a PM_4 cut-off point at 50% was attached to a cassette to isolate larger particles. The filters were subjected to acid digestion as a sample preparation step prior to analysis inductively coupled plasma mass spectrometry (ICP-MS). Coking phase had the highest number of particles with $2.20E^{+08} \pm 3.31E^{+07}$#/cm³ (48%), followed by flaming with $1.54E^{+08} \pm 8.60E^{+07}$#/cm³ (34 %) and ignition with $1.09E^{+08} \pm 3.38E^{+07}$#/cm³ (18 %). Submicron particles contributed the highest number concentration in all phases. Using mass concentration, coking had the highest contribution of 41.6± 15.0 µg/m³ (38.0%), ignition 35.5± 8.8 µg/m³ (32.4%) and flaming 32.3± 2.1 µg/m³ (30 %). Aluminium was the highest emitted element with $1.3E^{-01}$µg/m³ (43 %), followed by zinc $7.7E^{-02}$ µg/m³ (25 %), magnesium 7.0 E^{-02} µg/m³ (22 %) and chromium $1.4E^{-02}$µg/m³ (5%). The particle mode was more towards the smaller particle size bin. These particles have atmospheric radiation forcing and health implications. We detected toxic heavy metals such as Cd, Cr, Pb and Hg. These metal leads to various health complications as they do not have a safe threshold. The study suggests a comprehensive health risk assessment for workers exposed to emissions from charcoal burning activities to develop the best risk management strategies.

Keywords

physicochemical properties, elemental composition, emissions, combustion, particle size distribution

Introduction

In South Africa, the informal sector's contribution of 15–17% to employment highlights its importance in providing livelihoods and income for a significant portion of the population (ILO, 2019; Charman et al., 2019). Despite contributing about 5.2% to GDP, which is lower than in some other developing countries, the informal sector still plays a vital role in the economy, often serving as a buffer against unemployment and economic instability (Hogg, 2020). Demand for charcoal burning in Africa is increasing due to high-rise of electricity tariff, shortage of sufficient electricity, increased urbanization and slow growth of alternative clean energy sources (Bockarie et al., 2020). Charcoal is a commonly used energy source obtained from carbonized materials such as wood and coconuts shells (Ahmad et al., 2022). Wood is the most abundant material with a variety of wood species having high carbon content and low ash residues (Getahun et al., 2024). Low to middle income stakeholders mainly use solid fuel (charcoal) for fuel energy requirements for food preparation, as it is cheaper and said to be contributing unique flavour to the meat (Cova et al., 2022). Moreover, charcoal

© 2025. The Author(s). Published under a Creative Commons Attribution Licence.

burning produces less smoke than wood and coal (Ahmad et al., 2022). However, charcoal emissions are associated with the release of smaller particles, which contribute to poor air quality, climate change and health complications like upper respiratory diseases, lung cancer, heart diseases and neurological disorders (Ali et al., 2020. This is because of inhalation of small particulate matter in different size fractions from ($PM_{2.5}$, PM_4 and PM_{10}), toxic metals (lead, zinc, copper, vanadium, chromium, cobalt, cadmium, iron, selenium and arsenic) and other elements like magnesium, sodium, potassium, calcium and chloride (Kabir et al., 2011; Kopanakis et al., 2012).

The charcoal combustion process can be separated into three distinct phases, which are characterized by a variety of parameters (temperature, carbon monoxide (CO) and visible smoke). The ignition phase is usually the shortest process, lasting a few minutes, with highly visible smoke as the reaction between charcoal, fuel and air takes place. The flaming phase is mainly characterized by a highly visible flame, high temperature, and smoke, and lasts longer compared to ignition. The coking /smouldering phase is flameless, with hot amber-coloured charcoal and high CO emissions. The CO emission is also influenced by the ash layer on the surface of coal preventing oxygen from effectively reacting with the surface of charcoal carbon and resulting in more CO emission (Masekameni et al., 2018; Huang, Lee, and Wu, 2016a).

Despite this, studies have shown that to date, over 3 billion people globally rely on solid fuel as a basic energy source for cooking, space and water heating for low-income earners (Ezzati and Kammen, 2002). About 75% of the sub-Saharan African population is reliant on solid fuels like charcoal (Jelonek et al., 2020). Despite the high electrification rate in South Africa, there is still reliance on the use of charcoal amongst low-income dwellers or those in the informal economy (Masekameni et al., 2016; Balmer, 2007). There is little attention dedicated to field-based charcoal combustion emission characterisation as one of the air pollution sources (Bautista et al., 2009; Bhattacharya et al., 2002; Jolonek et al., 2020). Research focus has been directed to activities like coal burning for power generation that have emission control mechanisms (Susaya et al., 2010).

There have been many studies quantifying charcoal solid fuel combustion emissions from domestic devices through laboratory performance tests (in order to place such devices on the market) (Jelonek et al., 2020; Makonese et al., 2017; Masekameni et al., 2018; Kabir et al., 2005; Bautista et al., 2009). However, there is a paucity of information characterising emissions from charcoal burning activities in small-scale business enterprises in real-world use, despite increasing literature on the associated and toxicological impacts of exposure to PM and other pollutants (Kabir et al., 2011; Kocbach et al., 2005).

Charcoal users are exposed to xenobiotic emissions of gases and particulate matter at high concentrations in excess of the World Health Organization (WHO) recommended limits during cooking and space heating activities (North et al., 2019). There are several studies that confirm the association between charcoal emissions exposure and chronic health effects (Sana et al. 2019; Hussein et al., 2021), acute health effects (Owusu-Boadi et al., 2005; Juntarawijit et al., 2020; Das et al., 2017) and acute respiratory effects (Bautista et al., 2009; Admasie et al., 2018), but limited to household charcoal usage but little focus on informal food trading.

Diffuse emissions from charcoal burning activities outside laboratories in South Africa for advanced small-scale micro-enterprises such as food vending remains underreported. The underreporting of emissions from small combustion activities increases the uncertainties in geo-land mapping, emission inventory, air quality management, climate effects, environmental and health risk management. The detailed study of the physicochemical properties smoke particles, seeks to contribute to the limited available knowledge on smoke emissions from small-scale charcoal combustion activities. Data generated from this study may contribute to further understanding of interventions required to mitigate/prevent exposure in every step/phase of the combustion cycle namely, ignition, flaming and coking. To our knowledge, this may be amongst the few field-based study to assess the physicochemical properties of particles emitted from charcoal burning in South Africa.

Methodology

Description of the study area

The study was conducted in the City of Johannesburg, Fordsburg flea market (26°12′24″S 28°1′24″E), Region F in Fordsburg, west of Johannesburg (Figure 1). Johannesburg is home to 6, 2 million people (Statistics South Africa, 2023). The Fordsburg flea market is a semi-open structure facility with approximately 30 informal food traders and 16 traders in clothing and other consumables.

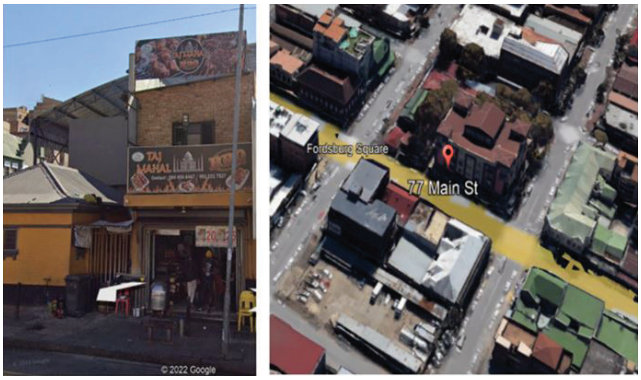


Figure 1: *Fordsburg flea market (Photo obtained from Google Earth Pro, 2024).*

Methodological approach

Apparatus

Nanozen DustCount 9000 (Nanozen Industries Inc, model 9000-Z1, Vancouver, Canada), real-time monitors were used to

© 2025. The Author(s). Published under a Creative Commons Attribution Licence.

monitor particle number concentration and mass concentration of particles during each phase cycle of the combustion cycle. The Nanozen is a direct-reading optical particle counter with 20 particle size bins ranging from 300 nm to 20 µm. It has a built-in cassette with a removable PVC 25 mm filter and a direct-reading optical particle counter for number and particle size quantification. Nanozen was selected as it provides an automated operation that reduces the effort of the researcher. The Nanozen monitoring device provides mass and number concentration as an output. This is an advantage since there will be no need to convert from mass to number concentration and vice versa.

Particles for studying the chemical properties were collected using a gravimetric sampling technique. The sampling train consisted of a Gilian Gilair 300plus, (Sensidyne, USA) pump, a Teflon tube, 37 mm cassette fitted with a 37 mm PVC membrane filter with a pore size of 5.0 µm and a $PM_{2.5}$ cyclone with a PM_4 cut-off point at 50% to isolate larger particles.

Pump calibration procedure

To ensure the correct pump flow rate before and after sampling, the two Gilian Gilair 300plus pumps underwent a flow calibration test. The calibration setup included a filter cassette, membrane filter, filter support pad, Teflon tubing, pump, soap dispenser, and a Gilibrator. Each pump was placed on a flat platform in the laboratory. The Gilibrator airflow was adjusted according to the manufacturer's instructions. The Teflon tube was connected from the pump inlet to the cassette outlet and from the cassette inlet to the Gilibrator outlet. A soap dispenser was used to introduce soap into the Gilibrator flow glass through the inlet. The pump was switched on, and the flow rate was set to 2.2 L/min. Soap was dispersed to measure the pump's airflow. This process was repeated three times before and after sampling. Once the pump flow and Gilibrator flow rate were matched, the pump was ready for sampling. The pre- and post-sampling flow rates were considered acceptable if the difference was within a 5% margin; otherwise, the data was discarded.

Air sampling

Sampling was conducted to capture and study the elemental composition of PM during different phases of combustion. Each phase was sampled using a uniquely identified filter attached to a cassette. PVC membrane filters were used to capture particles for the analysis of elements. PVC membrane filters are ideal in air monitoring for metals, silica and dust and their low moisture pickup makes it ideal for use in gravimetric analysis (Soo et al., 2016). These filters have proven to have a very high collection efficiency compared to other filters, especially for metals, dust, and silica (Soo et al., 2016). Emission from three food stalls were collected over three day period, with three combustion cycles sampled for each day. A total of 27 samples was therefore collected.

Monitoring arrangement

A Nanozen monitoring device was placed on a wooden surface platform away from high temperatures. A 1.5 meter long Teflon tube was attached to the Nanozen sampler and to the outlet of the Gilair sampling cassette. Particles were collected at 1.5 m height assuming the breathing circumference of a person carrying out braaiing activities (i.e. grilling) and 0.8 m away from the charcoal burning stove. The combustion conditions were divided into three phases viz. ignition, flaming and coking phase. The Nanozen monitoring device was switched on to match the duration of each combustion phase and a new cycle of measurements was carried out when a new combustion phase commenced. Three charcoal-burning stoves were monitored in triplicate. Each combustion phase was monitored in triplicates per combustion stove, for studying the particle number concentration, mass concentration and particle size distribution. The monitoring probe was placed on the same position for the duration of each combustion phase. The changes/transitioning from one phase to the next were noted with the change in characteristics (e.g. during flaming when the flame subsides and combustion station charcoal is amber, this was noted as end of flaming). The time was recorded as each phase ended and the next commenced. The instruments were set to collect particles every 10 seconds continually during each phase.

Sampling for chemical properties

Before sampling at the Fordsburg Flea Market, polyvinyl chloride (PVC) membrane filters of 37 mm in diameter and pore size of 5.0 µm were conditioned in a controlled laboratory environment over 24 hours. The filters were pre-weighed gravimetrically at the occupational health laboratory at the University of the Witwatersrand. Each filter was pre- and post-weighed 3 times and the average mass was taken. The weighing was done under laboratory conditions, after equilibrating at a temperature of 21 ± 2˚C and relative humidity 35 ± 2%) using an electronic microbalance scale, model CPA225D (Sartorius, AG, Göttingen, Germany) that has a minimum resolution of 0.001 mg. The weighing scale was calibrated at the Occupational Hygiene Laboratory, University of the Witwatersrand, using the internal function of the scale by pressing CAL option before weighing filters. Field blank filters were included for every sampling run (each day). These filters were not exposed to contaminants during sampling. These field blanks account for moisture gain/loss and possible contamination that might have taken place during the handling of filters (Parera et al., 2012). Each filter was exposed three times at each assigned combustion phase to collect sufficient particles for chemical analysis.

Final particle mass was calculated using Equation 1, while particle mass concentration was calculated using Equation 2.

$$\text{Final mass} = \text{ff}(\text{pm} - \text{prm}) + \text{fb}(\text{pm} - \text{prm}) \quad (1)$$

Where: ff is the field filter, fb is the field blank, pm is the post mass and prm is the pre mass.

$$\text{Concentration} = \frac{\text{m (µg)}}{\text{V (m}^3\text{)}} \quad (2)$$

M refers to the final mass calculated using a field blank. Final mass was calculated using Equation 1 and V is the volume of air.

© 2025. The Author(s). Published under a Creative Commons Attribution Licence.

Volume of air was determined using equation 3.

$$V = \frac{Fr(L/min)x\ t\ (\min)}{1000} \quad (3)$$

Where Fr is the pump flowrate in litres, t is time in minutes and 1000 is a conversion factor from litres to m^3.

Data analysis

Processing of Nanozen data

Nanozen data was extracted to a personal computer and data was analysed using Microsoft Excel software through graphical representations. This was done to determine the concentration, number and mass particle size distributions in all 3 phases (ignition, flaming and coking). The comparison was made between the phases to determine which phases contribute in terms of number and mass particle size distributions because of conditions pertaining during the monitoring period.

Inductively coupled plasma mass spectrometry (ICP-MS)

Elemental analyses were conducted at the University of the Witwatersrand, Chemistry Laboratory, Braamfontein campus, using a Perkin Elmer NexION 300 ICP-MS (Perkin Elmer, Waltham, MA, USA). Sample filters were folded and placed in pre-cleaned microwave digestion vessels, where 9 mL of suprapure nitric acid (HNO_3) and 1 mL of suprapure hydrogen peroxide (H_2O_2) (both from Merck) were added. A reagent blank was included in each batch as a control. The vessels were sealed and processed using a Mars 6 microwave digestion system.

Post-digestion, the samples were transferred to 50 mL volumetric flasks and diluted to the mark with 18.2 MΩ/cm² ultrapure water. Calibration standards of 0 µg/L, 0.1 µg/L, 0.5 µg/L, 1.0 µg/L, 5.0 µg/L, and 10 µg/L were prepared using 100 mg/L NIST traceable stock standards (Masekameni et al., 2020). Before analysis, the samples were filtered using 0.45 µm syringe filters and further diluted tenfold (1 mL diluted to 10 mL). The ICP-MS analysis procedure was also applied to a blank filter for quality control (Masekameni et al., 2020). The analyzed elements included manganese (Mn), magnesium (Mg), silicon (Si), lead (Pb), vanadium (V), cadmium (Cd), sodium (Na), iron (Fe), cobalt (Co), nickel (Ni), copper (Cu), chromium (Cr), and zinc (Zn). This method was adopted from a similar study on coal particle analysis (Chajduk and Paweł., 2023).

Statistical analysis

Statistical analysis was conducted to understand the underlying patterns and trends of the results. An F-test was conducted to test variances amongst compared phases, on particle number and mass concentration. T-test was conducted to compare mean differences between two compared phases. An alpha value of >0.05 indicates a test is not statistically significant, while an alpha value of <0.05 indicates a test that is statistically significant at 95% confidence interval (Zhao et al., 2024).

Results and discussion

Particle number, mass concentration and size bin distribution

In Table 1 we report the duration of individual combustion phase. The entire combustion cycle took about 134 minutes to complete. It must be noted that braaiing takes place the entire 8-hour shift in a day. Once one cycle is completed the operator decides to either start a new combustion cycle or refuel charcoal on the existing combustion process at the coking phase. In our study, operators were requested to allow the combustion cycle to complete and start a new one. The combustion phase duration comprised of triplicate measurements in a day, meaning the burning activities were carried out 3 times in a single monitoring and sampling campaign day.

Braaiing activities are only conducted at the coking phase once no visible flame can be observed. At this stage, it is anticipated that charcoal roast under sufficient temperature and oxygen. However, the braaiing activities at the coking phase leads to insufficient supply of oxygen, since the top part of the cooking platform is covered with raw chicken meat. The coking phase is also characterised by homogeneous heating generation and no visible smoke. The coking phase is the longest phase with over 63% of the time taken in a combustion cycle. The longer the coking phase may indicate adequate heating efficiency to sustain the braaiing activities. The ignition phase is the second longest combustion phase at about 22%. The ignition phase is reportedly associated with increased particulate and gaseous emissions. In a similar study where coal was an energy source ignition phase contributed the highest emissions of volatile organic compounds (Masekameni et al., 2018). Reducing the time taken to complete the ignition phase might lead to reduced emissions and increase the duration of the flaming (which can be used for space heating purposes) and coking phase for cooking and braaiing activities.

Table 1: *Duration of different combustion phases.*

	Ignition N = 3 per day	Flaming N = 3 per day	Coking N = 3 per day
Day 1	25 min	15 min	88 min
Day 2	30 min	22 min	75 min
Day 3	35 min	19 min	92 min
Average	**30 min**	**19 min**	**85 min**

The average particle number and mass concentration of each combustion phase are shown in Table 2. Particle number concentration for different combustion phases was determined. The coking phase contributed the most to the particle number concentration [($2.20E^{+08}$ ± $3.31E^{+07}$ (48%)], followed by the flaming phase at 34% and the ignition phase at 18%. This finding suggests that particle number concentration is directly proportional to the combustion progression. This is unlike other studies where the ignition phase and flaming phase often

© 2025. The Author(s). Published under a Creative Commons Attribution Licence.

release more particles than the coking phase, during which the combustion conditions are often homogeneous (Chen et al., 2019; Liu et al., 2017). In our study, an increase in the particle number concentration might have been influenced by the introduction of chicken pieces being placed on the braaiing stand. When meat was introduced, there was an observable white plume for a few minutes the meat was removed. This might be due to the evaporation of the moisture contained in the meat and the liquid spice that was used to soak the meat as a flavour. A study by Fix et al. (2013) suggested that the solid-to-particle process caused by high-temperature exposure from charcoal heat causes mechanisms such as bubble bursting of particles and phenomena of surface ash shedding, which also contribute to a high number concentration, especially during the coking phase and flaming.

Table 2: *Average (± 1 standard deviation) of particle number and mass concentration per phase.*

Combustion Phase	Mass concentration		Number concentration	
	(µg/m³)	%Contribution	#/cm³	%Contribution
Ignition	35.5± 8.8	32	$8.23E^{+07}$ ± $3.38E^{+07}$	18
Flaming	32.3± 2.1	30	$1.54E^{+08}$± $8.60E^{+07}$	34
Coking	41.6± 15.0	38	$2.20E^{+08}$ ± $3.31E^{+07}$	48

Figure 2(a) shows the average particle number concentration per combustion phase, ranging from $8.23E^{+07}$ to $2.20E^{+08}$ (#/m³). Coking contributed the highest number followed by flaming and ignition respectively. In Figure 2 we report the average mass and particle number concentration at each combustion phase. In Figure 2(a), particle number concentration increases as the combustion process progresses. This finding is similar to other studies that reported high particle number concentration as combustion progresses (Masekameni et al., 2018; Tiwari et al., 2014). According to Susaya et al. (2010), the coking phase in combustion takes the longest compared to ignition and flaming. The extended duration in the coking phase results in a greater impact on the overall combustion process. A similar study on barbecue activities found that the duration of combustion phases significantly affects both the number and mass concentration of emissions (Zhang et al., 2014; Tiwari et al., 2014). In Figure 2(b), a decline in mass concentration can be seen between the ignition phase and the flaming/ coking phase. Although the ignition phase produced the smallest number of particles compared to the flaming and coking phase, the mass concentration was found to be higher. A higher mass concentration at the ignition phase might be due to the release of larger particles compared to smaller particles produced during the flaming phase as heat increases. The coking phase has the highest mass concentration, which might be due to the introduction of meat that then releases smaller droplets as water vapour. This finding is contrary to a previous study, which reported lower mass concentration at the coking phase (Guo et

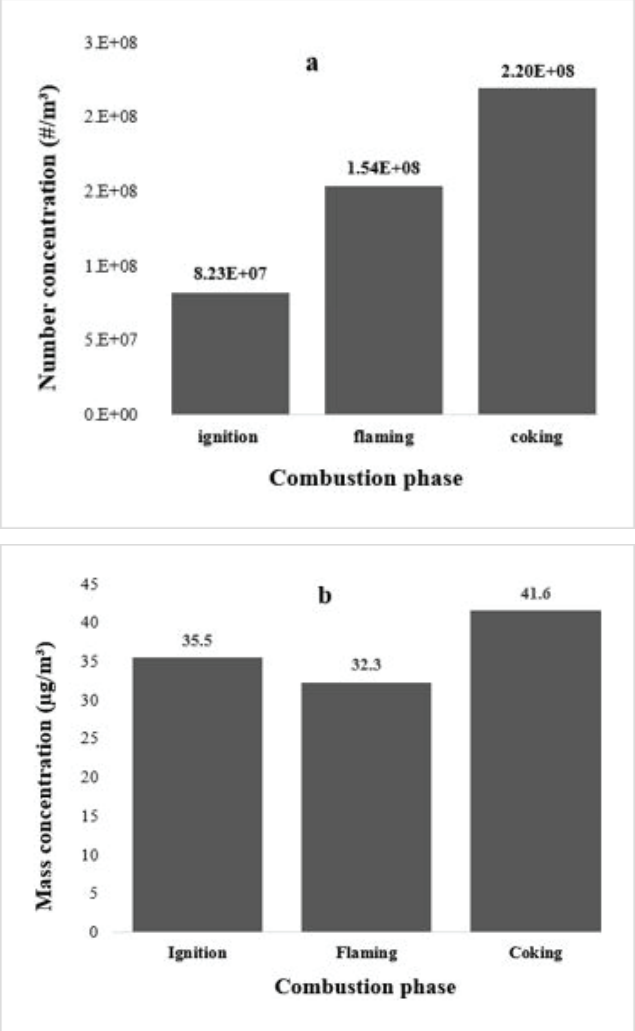


Figure 2: *Average particle number (a) and mass concentration (b) per combustion phase.*

al., 2018). In the case of our study adding to the introduction of meat on a braaiing panel there are variety of sources added. Major ingredients of barbeque sources included vinegar, salt, sugar, salt and water.

The major ingredients of BBQ sauce are soy sauce, vinegar and occasionally sesame oil and hot pepper. When burning ingredients, there was an observable plume suggesting an increase of particulate matter and gases. A similar finding was reported in a charcoal burning study by Buttacharyia et al. (2002) who indicated that burning of oil and dipping sauce contributes to increased emissions of PM and gases.

The increase in particles emitted during the coking phase is a result of an increase in temperature within the coal (Huang et al., 2016). In this study, ignition has the second highest mass concentration at 35.5 µg/m³ as evident in Figure 2(b). At this stage, char structures break and start to release tar-containing moisture during the initial evaporation process. The flaming phase is associated with an increase in temperature and fine particle emissions. This explains why the flaming phase has a

© 2025. The Author(s). Published under a Creative Commons Attribution Licence.

lower mass concentration at 32.3 µg/m^3. During flaming, the char structure would have released all moisture have no effect on the density of particles, while during the coking phase there is the highest mass concentration of particles of 41.6 µg/m^3 of 11.65 µg/m^3. Moreover, during braaiing activity, the fat and liquid in the meat also contribute to the density of released particles. This makes them heavier even though the phase has the highest number of small particles.

Table 3: *Particle number per combustion phases statistical analysis.*

Combustion phase	Average particle number conc (#/m^3) & Standard deviation	F-Test	P-value	Sig @ 95% Yes/No
Ignition vs	1.09E^{+08} ± 3.38E^{+07}	0.267	0.535	No
Flaming	1.54E^{+08} ± 8.60E^{+07}			
Ignition vs	1.09E^{+08} ± 3.38E^{+07}	0.981	0.030	Yes
Coking	2.20E^{+08} ± 3.31E^{+07}			
Flaming vs	1.54E^{+08} ± 8.60E^{+07}	0.259	0.366	No
Coking	2.20E^{+08} ± 3.31E^{+07}			

Three possible pairings of the particle number concentration emitted from the three combustion phases results are presented in Table 3. From the results, there was only one pairing with statistically significant difference. This finding is contrary to Makonese et al. (2017), where it was found that emissions significantly reduce as combustion conditions change. However, the study by Makonese et al. (2017) focused on coal, not charcoal. Additionally, the reporting matrix was mass concentration, while our study reports on number concentration.

Particle number and mass concentration per particle size bin

Figure 3 (a & b) shows the average particle number and mass concentration per particle size bin of each phase. When using a number concentration matrix it can be seen in Figure 3a that most particles released are smaller in diameter irrespective of the combustion phase. The particle mode is likely to be less than 1 micrometre. In Figure 3(b) the particle mass shifts towards a larger mode around PM_4. This finding was expected since smaller particles, although present in larger numbers, have a lower mass. Larger particles might be low in terms of number concentration compared to smaller particles, but using the mass matrix as a unit of expression, they might be high in concentration. In contrast, the particle number concentration for smaller particles is often higher compared to larger particles. Our findings are similar to other studies (Tiwari et al., 2014; Torvela et al., 2014).

Results obtained from this study show that the particle number concentration has a left-skewed distribution, with a long tail to the right, suggesting that majority of the particles are of smaller diameter (Figure 3a), while the mass concentration showed a right-skewed distribution, suggesting that the highest mass is produced by larger particles, see Figure 3b. This finding is

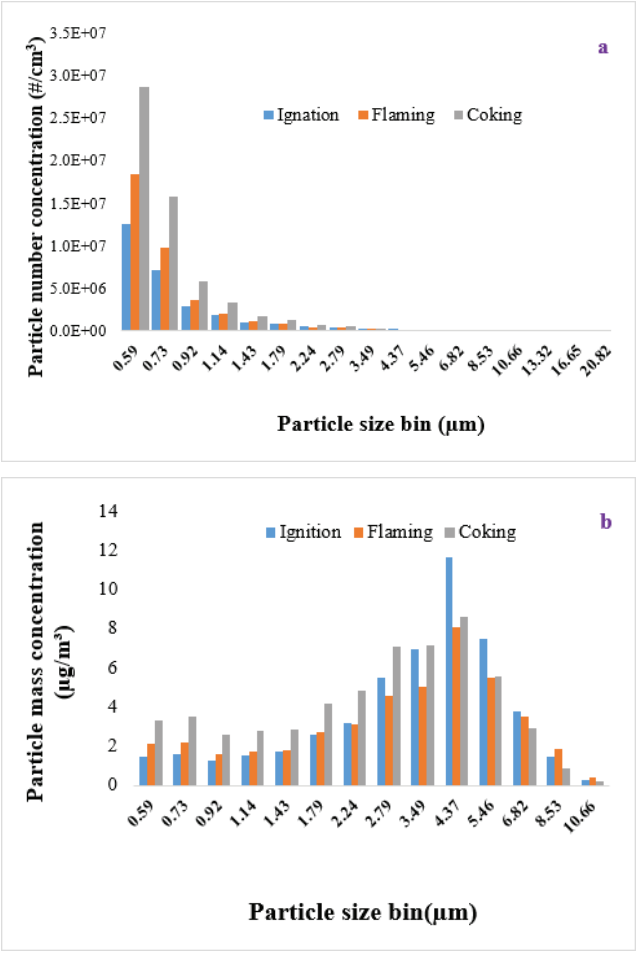


Figure 3: *Particle number (a) and mass (b) concentration per particle size bin for three combustion phases.*

worrying because most occupational exposure limits are based on mass, but little consideration is given to particle number concentration. Emerging scientific literature suggests that the toxicity of a chemical compound is based on the number of particles, surface area and diameters. Smaller particles tend to have a higher residence time in the breathing zone and can easily penetrate to the lower respiratory system and translocate to vital organs during the gaseous exchange process (Morawska & Buonanno, 2021).

The ignition phase contributed the highest number of large particles as shown in Figure 3(b). This can be attributed to the combustion process where there is fragmentation of charcoal into small fractions as temperature increases. The flaming phase also showed an increase in larger particles as shown in Figure 3(b), similar to findings by Masekameni et al. (2018). This may be because of particle coagulation and agglomeration of smaller particles. However, unlike in a laboratory experimental set-up, the transition from the ignition phase to the flaming phase is difficult to accurately time and control. It can be anticipated that larger particles should be associated with the ignition phase due to lower temperature and smouldering combustion conditions. The coking had the least number of larger particles, but it showed a presence of coarse particles with aerodynamic

© 2025. The Author(s). Published under a Creative Commons Attribution Licence.

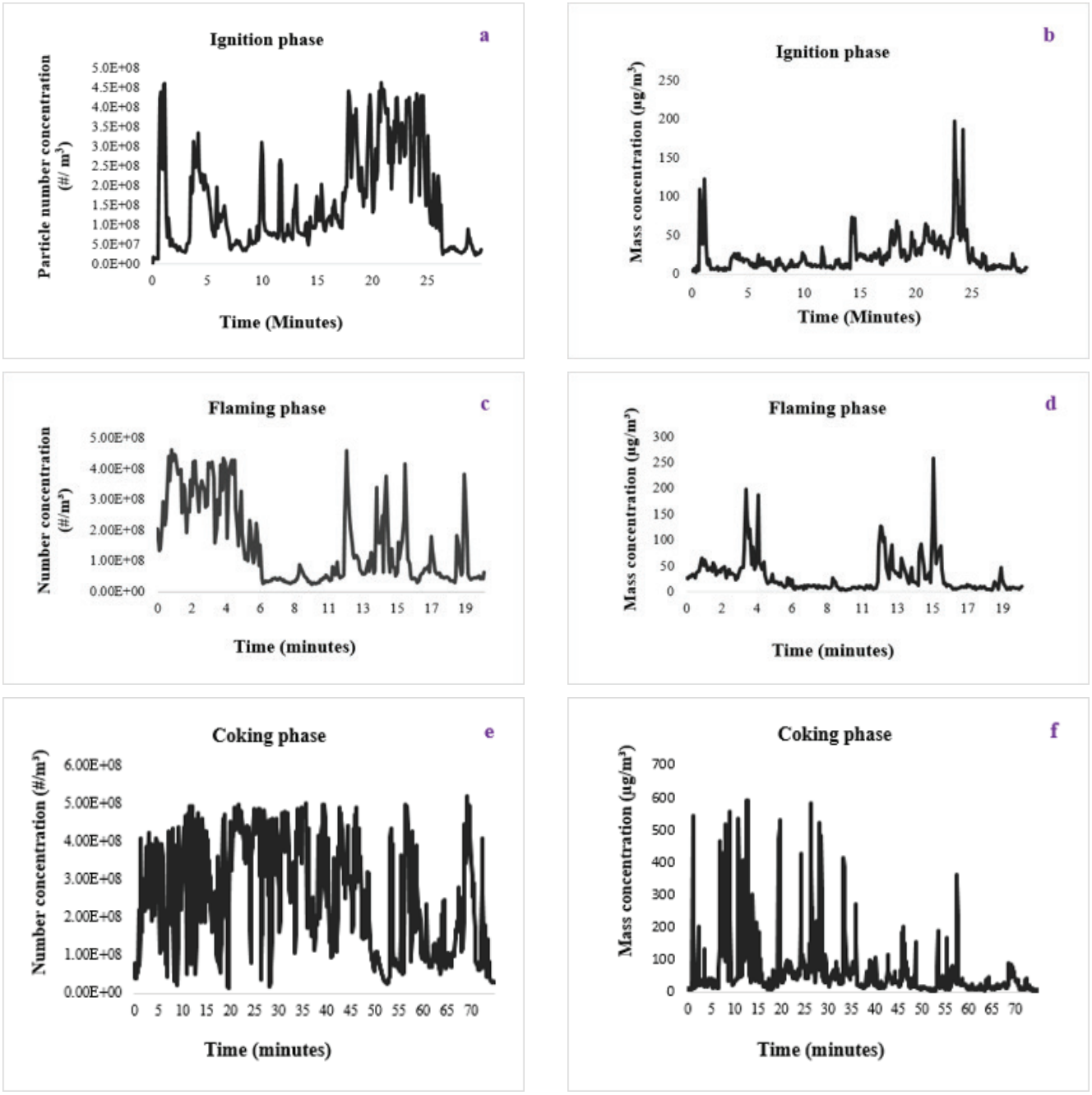


Figure 4 (a-f): *Particle number and mass concentration time series.*

diameter of 13.32 µm. This can be attributed to the leaking of oil from the meat, which could have re-suspended larger particles. It is important to note that the coking phase on average contributed the highest number of ultrafine particles because of homogenous combustion conditions, followed by flaming phase and ignition phase respectively.

Particle number and mass concentration real-time series plot

Time series plots showing particle number and mass concentration for the different combustion phases are presented in Figure 4 (a-f). In Figure 4 (a-b), as particle number increases, the particle mass is seen to increase. At this stage, most of the larger particles are emitted as the combustion conditions are yet stabilised. This phase is associated with low-temperature conditions and an insufficient supply of combustion air. In Figure 4 (c-d), the flaming phase shows an inconsistent emission profile. This was expected as combustion conditions improve, more of the smaller particles are expected to be released, hence lower mass. The coking phase in Figure 4 (e-f) presented a different emissions profile from the literature (Makonese et al., 2017), who found that emissions of particulate matter were highest during the first hour of combustion followed by flaming with the least emissions emitted during the smouldering or coking phase. However, this study used coal instead of charcoal. Moreover, there was no introduction of meat during the coking

© 2025. The Author(s). Published under a Creative Commons Attribution Licence.

phase but only water boiling in a 10 L pot was performed. It was anticipated, as guided by the literature, that fewer particles will be emitted at this stage (Tiwari et al., 2014). During the coking phase, most volatiles are driven out and char burns in sufficient oxygen. The residual emissions expected at this phase are often fly ash. However, the study suggests that an increase in particle mass and number concentration is influenced by the introduction of meat on the braaiing platform. As meat is placed on the braaiing platform, there was dripping of water from sauces used as ingredients to flavour the meat and a limitation of oxygen supply to the fuel-bed.

From observations regarding particle number and mass concentration as shown in Figure 4 (a-b) on the real-time series plot, there is a spike in number concentration (maximum of $4.5E^{+08}$ #/m^3) and mass concentration (maximum of 130 µg/m^3) between 0 – 5 minutes during ignition. At the end of the ignition phase between 20 – 25 minutes (max $4.5E^{+08}$ #/cm^3 for number and max 200 µg/m^3 for mass concentration). The spike in concentration subsides after 26 minutes to about $5.0E^{+07}$ #/cm^3 and 20 µg/m^3 for mass concentration. For the flaming phase as shown in Figure 4 (c), there is an immediate spike in number concentration from 0 – 5 minutes and peaks again at about 12 – 19 minutes which is the end of the phase. For mass concentration as shown in Figure 4 (d), there is a delay in spikes and this only peaks at about 3 minutes to 5 minutes from around 60 µg/m^3 to 200 µg/m^3, and again at about 12 – 15 minutes at 250 µg/m^3. However, the mass is reduced towards the end of the flaming phase to around 10 µg/m^3.

Reduction in mass concentration may be attributable to improved combustion conditions at the end of the phase when the flame subsides and the char is amber with no visible flame or smoke. The small particles are mainly released during flaming transitioning into the coking phase. This can also be observed from the number concentration history, which peaked at the end of the phase, meaning it was the peak of smaller particles. With the coking phase there was a regular spike in both number and mass concentration from the start of the phase till the end as shown in Figure 4 (e-f). The consistent spikes during the coking phase can be attributed to the leaking of oil and spices. This is possible as a result of the limitation of oxygen supply for homogenous combustion conditions (Boman, 2003).

Elemental composition

In Table 4, we have shown all elements detected, their mass concentration, and the percentage contribution of each element that was analysed in different combustion phases. The elements detected were Mg, Al, V, Cr, Co, Ni, Cu, Zn, As, Se, Cd, Hg and Pb (Table 4). The fuel analysis of the charcoal used in this restaurant showed the following elemental contents Mn, S, P, Si, Cr, Ni, Mg, Ca, Fe, Cu, Al, V, B and Pb. Metals identified were categorised into transition metals: Mn, Cr, Ni, Fe, Cu, V; alkaline Earth Metals: Mg, Ca; post-transition metals: Pb, Al and Nonmetals: S, P, Si and, B. Transitional metals were found to be contributing the highest mass. Al had the highest mass concentration $1.3E^{-01}$ µg/m^3 with 43 % contribution as shown in Table 4. Higher Al emissions can be due to the decaying of the aluminium produced grilling plates not necessarily from charcoal. Additionally, the use of aluminium foils during meat grilling can also contribute to Al emissions. Taner et al. (2013) also found these metals in abundance with Al being the highest, followed by Mg with the contribution of 22 %. The element with the second highest concentration in this study was Zn [$7.4E^{-02}$ µg/m^3 (25 %)], similarly to findings by Susaya et al. (2010) which found Zn to be contributed the highest concentration.

A trace elements such as Se is associated with various forms of ecosystem and human health toxicity. Although in our study Se was found to be among the least of emitted elements, chronic exposure even at low dosages may cause Se poisoning (Song et al., 2020). Some toxic heavy metals were released during charcoal burning with severe toxic effects at certain thresholds. We found traces of Cr, Pb, and Cd, while it was below the limit of quantification (<0.0001 µg/m^3). Notably however, certain heavy metals including As, cadmium (Cd), lead (Pb), mercury (Hg), and chromium (Cr)(VI) are non-threshold toxins, meaning they can cause harm even at low concentrations. Given the toxicity of these metals, they are ranked among the highest priority metals (Tchounwou et al., 2012). In the renal system, high-dose acute exposure to chromium (Cr (VI)) can lead to tubular necrosis and renal failure. In contrast, low-dose chronic exposure is generally associated with transient renal effects (ATSDR 2012).

Table 4: *Average elemental composition mass concentration per combustion phase.*

Element	Ignition Mass conc. (µg/m^3)	%Contr.	Flaming Mass conc. (µg/m^3)	%Contr.	Coking Mass conc. (µg/m^3)	%Contr.
Mg	0.0902	28.8	0.0462	17.8	0.0735	20.2
Al	0.1205	38.4	0.1090	42.1	0.1731	47.5
V	0.0009	0.3	0.0008	0.3	0.0009	0.3
Cr	0.0111	3.5	0.0154	5.9	0.0158	4.3
Co	0.0008	0.3	0.0006	0.2	0.0006	0.2
Ni	0.0060	1.9	0.0071	2.7	0.0055	1.5
Cu	0.0055	1.8	0.0047	1.8	0.0043	1.2
Zn	0.0733	23.4	0.0718	27.7	0.0850	23.3
As	0.0009	0.3	0.0010	0.4	0.0010	0.3
Se	0.0013	0.4	0.0004	0.2	0.0023	0.6
Cd	0.0008	0.2	0.0008	0.3	0.0008	0.2
Hg	0.0001	0.0	0.0000	0.0	0.0001	0.0
Pb	0.0020	0.6	0.0013	0.5	0.0018	0.5

In a recent study, elements such as selenium (Se), arsenic (As), and vanadium (V) are primarily associated with meat grilling. However, our study found contrary results (Leite et al., 2020). We observed that higher concentrations of these elements were present in all three combustion phases.

© 2025. The Author(s). Published under a Creative Commons Attribution Licence.

Conclusion

Emissions profiles in a meat-braaiing flea market using charcoal as a primary source of energy were studied. The study assessed the particle size distribution of emitted particles, particle number concentration, mass concentration and chemical properties. The particle size distribution indicated a left-skewed data, suggesting that most of the particles were of smaller diameter when using a number concentration matrix. However, the mass distribution was skewed to the right suggesting larger particle mass of particles above PM_4. Most of the particles were emitted during the coking phase with the ignition emitting the least particles. The mass concentration showed a left distribution suggesting that the highest mass is produced by larger particles. This finding is worrying since most occupational exposure limits are only limited to mass concentrations as a unit of measure. Smaller particles have been reportedly associated with high lung deposition efficiency. Once deposited in the lower respiratory tract they dislocate to other vital organs. We have found traces of toxic heavy metals in all three combustion phases. Toxic heavy metals such as Cr, Pb, Se, Cd and Hg cause various forms of ill-health even at low dosages. Our study suggests that certain properties of fire-emitted particulate matter (PM) such as the combustion phase (ignition, flaming and coking) of charcoal burning must be considered to identify significant high emissions points. Consequently, to date, there has been little consideration made in the literature to use combustion phase indicators in emissions evaluation.

Acknowledgement

Sincere appreciation goes to Mr Makae, Lebogang Phama and Dr Goitsemang Keretetse for their assistance during field experiments and to Mr Philip Pieterse for assisting with ICP-MS analysis. Many thanks to Mphidiseng Zwane for assisting with sample analysis payment.

Author contributions

Khumalo and Masekameni conceptualized and prepared the manuscript. Khumalo also experimented and wrote the first draft of the paper. Masekameni developed the methodology for coal emission capturing and analysis. He further supervised the sampling of particulate matter, data analysis, interpretation, and the presentation of arguments, and assisted in the editing of the manuscript. Rathebe and Khumalo assisted with the manuscript structure and write-up. Rathebe did the final validation of the study methodology.

References

Admasie A, Kumie A, Worku A. (2018). Children under five from houses of unclean fuel sources and poorly ventilated houses have higher odds of suffering from acute respiratory infection in Wolaita-Sodo, Southern Ethiopia: A Case-Control Study. J Environ Public Health. 2018(1). https://doi.org/10.1155/2018/9320603.

Ahmad, R.K., Sulaiman, S.A., Yusup, S., Dol, S.S., Inayat, S., Umar, H.A. (2022). Exploring the potential of coconut shell biomass for charcoal production. Ain Shams Engineering Journal, 13(1). https://doi-org.uplib.idm.oclc.org/10.1016/j.asej.2021.05.013.

Ali, N., Adil, I., Magsi, A., Asif, E. (2020) Particle size, morphology and characterization of indoor and outdoor airborne particulate matter for toxic metals in Karachi. Int. J. Environ. Sci. Technol. 17, 3969–3982. https://doi-org.uplib.idm.oclc.org/10.1007/s13762-020-02771-4.

ATSDR (2007) Toxicological profile for lead. Agency for Toxic Substances and Disease Registry. http://www.atsdr.cdc.gov/toxprofiles/tp13.pdf

Balmer, M. (2007). Household coal use in an urban township in South Africa. Journal of Energy in Southern Africa, 18(3), 27–32. https://doi.org/10.17159/2413-3051/2007/v18i3a3382.

Bautista, L.E., Correa, A., Baumgartner, J., Breysse, P., Matakoski, G.M. (2009). Indoor charcoal smoke and acute respiratory infections in young children in the Dominican Republic. American Journal of Epidemiology, 169(5), 572–80. https://doi.org/10.1093/aje/kwn372.

Bhattacharya, S., Albina, D. and Khaing, A.M. (2002). Effects of selected parameters on performance and emission of biomass-fired cookstoves. Biomass and Bioenergy, 23(5), 387–395. https://doi.org/10.1016/S0961-9534(02)00062-4.

Boman, B.C., Forsberg, A.B., Järvholm, B.G. (2003). Adverse health effects from ambient air pollution in relation to residential wood combustion in modern society. Scand J Work Environ Health, 29(4), 251-260. https://doi.org/10.5271/sjweh.729.

Charman, A., Bacq, S., Brown, K. (2019) Spatial determinants of formal retailers' impact on informal microenterprises in the township context: A case study of Philippi East, Cape Town, Food Security SA Research Report Series. Research Report 002. DST-NRF Centre of Excellence in Food Security, Cape Town.

Chen, Y., Kong, S., Yan, Q., et al. (2019). Size-segregated emission factors and health risks of PAHs from residential coal flaming/smoldering combustion. Environ Sci Pollut Res Int., 26(31), 31793–31803. https://doi-org.uplib.idm.oclc.org/10.1007/s11356-019-06340-2.

Cova, C.M., Rincón, E., Espinosa, E., Serrano, L., Zuliani, A. (2022). Paving the way for a green transition in the design of sensors and biosensors for the detection of volatile organic compounds (VOCs). Biosensors, 12 (2). https://doi.org/10.3390/bios12020051.

Chajduk E, Kalbarczyk P. (2023). Comparison of the analytical performance of Inductively Coupled Plasma Mass Spectrometry and Instrumental Neutron Activation analysis techniques in the

© 2025. The Author(s). Published under a Creative Commons Attribution Licence.

elemental analysis of coal fly ash. Minerals, 13(12). https://doi.org/10.3390/min13121484.

Das, I., Jagger, P., Yeatts, K. (2017) Biomass cooking fuels and health outcomes for women in Malawi. EcoHealth, 14, 7–19. https://doi-org.uplib.idm.oclc.org/10.1007/s10393-016-1190-0.

Ezzati, M., Kammen, D. M. (2002). the health impacts of exposure to indoor air pollution from solid fuels in developing countries: knowledge, gaps, and data needs. Environ Health Perspect., 110 (11), 1057 – 1068. https://doi.org/10.1289/ehp.02110105.

Fix, G., Seames, W., Mann, M., Benson, S., Miller, D. (2013). The effect of combustion temperature on coal ash fine-fragmentation mode formation mechanisms. Fuel, 113, 140–147. https://doi.org/10.1016/j.fuel.2013.05.096.

Getahun, Z., Abewaa, M., Mengistu, A., et al., (2024). Towards sustainable charcoal production: Designing an economical brick kiln with enhanced emission control technology. Heliyon, 10(6). https://doi.org/10.1016/j.heliyon.2024.e27797.

Guo, F., Ju, Y., Wang, G., Alvarado, E.C., Yang, X., Ma, Y., Liu, A. (2018). Inorganic chemical composition of PM2.5 emissions from the combustion of six main tree species in subtropical China. Atmospheric Environment, 189, 107–115. https://doi.org/10.1016/j.atmosenv.2018.06.044.

Hogg, A. (2020), GG Alcock: time to recognise millions in SA's flourishing informal economy, BizNews, 22 Aug 2019. https://www.biznews.com/good-hope-project/gg-alcock-recognise-informal-economy

Huang, H. L., Lee, W. M. G., Wu, F. S. (2016). Emissions of air pollutants from indoor charcoal barbecue. Journal of Hazardous Materials, 302, 198–207. https://doi.org/10.1016/j.jhazmat.2015.09.048.

Hussein, H., Shamsipour, M., Yunesian, M., et al. (2021). Fuel type use and risk of respiratory symptoms: A cohort study of infants in the Northern region of Ghan. Sci Total Environ, 755(1). https://doi.org/10.1016/j.scitotenv.2020.142501.

OECD/ILO. (2019). Tackling Vulnerability in the Informal Economy, Development Centre Studies; OECD Publishing: Paris, France. https://www.oecd.org/en/publications/tackling-vulnerability-in-the-informal-economy_939b7bcd-en.html.

Jelonek, Z., Drobniak, A., Mastalerz, M., Jelonek, I. (2020). Environmental implications of the quality of charcoal briquettes and lump charcoal used for grilling. Science of The Total Environment, 747. https://doi.org/10.1016/j.scitotenv.2020.141267.

Juntarawijit, C., Juntarawijit, Y. (2020). Cooking with Biomass fuel and cardiovascular disease: a cross-sectional study among rural villagers in Phitsanulok, Thailand. F1000Research, 9:307. https://f1000research.com/articles/9-307/v2.

Leite, L.C.S., Melo, E.S.P., Arakaki, D.G., Dos Santos, E.F., do Nascimento, V.A. (2020). Human Health Risk Assessment through Roasted Meats Consumption. Int. J. Environ. Res. Public Health, 17(18). https://doi.org/10.3390/ijerph17186737.

Liu, C., Zhang, C., Mu, Y., Liu, J., Zhang, Y. (2017). Emission of volatile organic compounds from domestic coal stove with the actual alternation of flaming and smoldering combustion processes. Environmental Pollution, 221, 385-391. https://doi.org/10.1016/j.envpol.2016.11.089.

Kabir, E., Kim, K. H., Yoon, H. O. (2011). Trace metal contents in barbeque (BBQ) charcoal products. Journal of Hazardous Materials, 185(2–3), 1418–1424. https://doi.org/10.1016/j.jhazmat.2010.10.064.

Kocbach, A., Johansen, B. V., Schwarze, P. E., Namork, E. (2005). Analytical electron microscopy of combustion particles: A comparison of vehicle exhaust and residential wood smoke. Science of the Total Environment. 346(1–3), 231–243. https://doi.org/10.1016/j.scitotenv.2004.10.025.

Kopanakis, I., Eleftheriadis, K., Mihalopoulos, N., Lydakis-Simantiris, N., Katsivela, E., Pentari, D., Zarmpas, P., Lazaridis, M. (2012). Physico-chemical characteristics of particulate matter in the Eastern Mediterranean. Atmospheric Research, 106, 93–107. https://doi.org/10.1016/j.atmosres.2011.11.011.

Makonese, T., Masekameni, D.M., Annegarn, H.J., Forbes, P.B.C. (2017) Emission factors of domestic coal-burning braziers. South African Journal of Science, 113(3/4). https://doi.org/10.17159/sajs.2017/20160187.

Masekameni, D.M., Brouwer, D., Makonese, T., Rampedi, I.T., Gulumian, M. (2018). Size distribution of ultrafine particles generated from residential fixed-bed coal combustion in a typical brazier. Aerosol Air Qual. Res., 18, 2618-2632. https://doi.org/10.4209/aaqr.2018.03.0105.

Masekameni, D. M., Makonese, T., Annegarn, H.J. (2016). Performance evaluation of three charcoal stoves. Proceedings of the 24th Conference on the Domestic Use of Energy, Cape Town, South Africa. https://doi.org/10.1109/DUE.2016.7466702.

Masekameni, D.M., Andraos, C., Yu, I. J., Gulumian, M. (2022). Exposure Assessment of Silver and Gold Nanoparticles Generated During the Synthesis Process in a South African Research Laboratory. Frontiers in Toxicology, 4. https://doi.org/10.3389/ftox.2022.892703.

Masekameni, M.D., Makonese, T., Rampedi, T.I., Keretetse, G.S. (2020). Morphology and elemental analysis of freshly emitted

© 2025. The Author(s). Published under a Creative Commons Attribution Licence.

particles from packed-bed domestic coal combustion. Clean Air Journal, 30(2). https://doi.org/10.17159/caj/2020/30/2.8582

Morawska, L., Buonanno, G. (2021). The physics of particle formation and deposition during breathing. Nature Reviews Physics, 3, 300–301. https://doi-org.uplib.idm.oclc.org/10.1038/s42254-021-00307-4.

Musara, M., Nieuwenhuizen, C. (2020). Informal sector entrepreneurship, individual entrepreneurial orientation and the emergence of entrepreneurial leadership. Africa Journal of Management, 6(3):194–213. https://doi-org.uplib.idm.oclc.org/10.1080/23322373.2020.1777817.

North, C.M., MacNaughton, P., Lai P.S., et al. (2019). Personal carbon monoxide exposure, respiratory symptoms, and the potentially modifying roles of sex and HIV infection in rural Uganda: a cohort study. Environ Health, 18(1). https://doi-org.uplib.idm.oclc.org/10.1186/s12940-019-0517-z.

Owusu-Boadi, K., Kuitunen, M. (2006). Factors affecting the choice of cooking fuel, cooking place and respiratory health in the Accra metropolitan area, Ghana. J Biosoc Sci., 38(3), 403–412. https://doi.org/10.1017/S0021932005026635.

Sana, A., Meda, N., Badoum, G., et al. (2019) Primary cooking fuel choice and respiratory health outcomes among women in charge of household cooking in Ouagadougou, Burkina Faso: cross-sectional study. Int J Environ Res Public Health. 16(6). https://doi.org/10.3390/ijerph16061040.

Sekine, Y., Sakajiri, K., Kikuchi, E., Matsukata, M. (2008). Release behavior of trace elements from coal during high-temperature processing. Powder Technology, 180(1–2), 210–215. https://doi.org/10.1016/j.powtech.2007.03.012.

Song, G., Xu, W., Liu, K., Song, Q. (2020). Transformation of selenium during coal thermal conversion: Effects of atmosphere and inorganic content. Fuel Processing Technology, 205. https://doi.org/10.1016/j.fuproc.2020.106446.

Soo, J. C., Monaghan, K., Lee, T., Kashon, M., Harper, M. (2016). Air sampling filtration media: Collection efficiency for respirable size-selective sampling. Aerosol Sci Technol., 50(1), 76–87. https://doi.org/10.1080/02786826.2015.1128525.

Stats SA Department: Statistics South Africa (2023). Sustainable Development Goals: Country Report 2023. Available at: www.statssa.gov.za.

Susaya, J., Kim, K. H., Ahn, J. W., Jung, M. C., Kang, C. H. (2010). BBQ charcoal combustion as an important source of trace metal exposure to humans. Journal of Hazardous Materials, 176(1–3), 932–937. https://doi.org/10.1016/j.jhazmat.2009.11.129.

Taner, S., Pekey, B., Pekey, H. (2013). Fine particulate matter in the indoor air of barbeque restaurants: Elemental compositions, sources and health risks. Science of the Total Environment, 454–455, 79–87. https://doi.org/10.1016/j.scitotenv.2013.03.018.

Tchounwou, P.B., Yedjou, C.G., Patlolla, A.K., Sutton, D.J. (2012). Heavy Metal Toxicity and the Environment. In: Luch, A. (eds) Molecular, Clinical and Environmental Toxicology. Experientia Supplementum, vol 101. Springer, Basel. https://doi-org.uplib.idm.oclc.org/10.1007/978-3-7643-8340-4_6

Tiwari, M., Sahu, S.K., Bhangare, R.C., Yousaf, A., Pandit, G.G. (2014). Particle size distributions of ultrafine combustion aerosols generated from household fuels, Atmospheric Pollution Research, 5(1), 145–150. https://doi.org/10.5094/apr.2014.018.

Torvela, T., Tissari, T., Sippula, O., Kaivosoja, T., Leskinen, J., Virén, A., Lähde, A., Jokiniemi, J. (2014). Effect of wood combustion conditions on the morphology of freshly emitted fine particles, Atmospheric Environment, 87, 65–76. https://doi-org.uplib.idm.oclc.org/10.1016/j.atmosenv.2014.01.028.

Wilschefski, S. C., Baxter, M. R. (2019). Inductively Coupled Plasma Mass Spectrometry: Introduction to Analytical Aspects. Clin Biochem Rev., 40(3), 115–133. https://doi.org/10.33176/AACB-19-00024.

Zhang T., Wooster M.J., Green D.C., Main B. (2014). New field-based agricultural biomass burning trace gas, PM2.5, and black carbon emission ratios and factors measured in situ at crop residue fires in Eastern China. Atmospheric Environment, 121, 22–34. https://doi.org/10.1016/j.atmosenv.2015.05.010.

Zhao G., Yang J., Zhang L., Yang H. (2024). ANOVA F Test of Non-Null Hypothesis. European Journal of Statistics, 4(2024). https://doi.org/10.28924/ada/stat.4.4.

© 2025. The Author(s). Published under a Creative Commons Attribution Licence.